THE JOURNAL OF BIOLOGICAL CHEMISTRY
Vol. 274, No. 10, Issue of March 5, pp. 6586–6593, 1999

Printed in U.S.A.

Distinct Structural Attributes Regulating von Willebrand Factor A1 Domain Interaction with Platelet Glycoprotein Ibα under Flow*

(Received for publication, December 2, 1998)

Shigeki Miyata‡ and Zaverio M. Ruggeri§

From the Roon Research Center for Arteriosclerosis and Thrombosis, Division of Experimental Hemostasis and Thrombosis, Departments of Molecular and Experimental Medicine and of Vascular Biology, The Scripps Research Institute, La Jolla, California 92037

We have used recombinant von Willebrand factor (vWF) fragments to investigate the properties regulating A1 domain interaction with platelet glycoprotein (GP) Ibα. One fragment, *r*vWF$^{508–704}$, represented the main portion of domain A1 (mature subunit residues 497–716) within the Cys^{509}-Cys^{695} disulfide loop. The other, *r*vWF$^{445–733}$, included the carboxyl-terminal region of domain D3, preceding A1, and corresponded to the proteolytic fragment originally identified as the GP Ibα-binding site (residues 449–728). Conformational changes were induced by reduction and alkylation of the Cys^{509}-Cys^{695} bond and/or exposure to acidic pH. The cyclic *r*vWF$^{445–733}$ fragment exhibited the function of native vWF A1 domain. When immobilized onto a surface, it tethered platelets at shear rates up to 6,300 s^{-1} mediating low velocity translocation but not stable attachment; in solution, it exhibited limited interaction with GP Ibα. In contrast, fragments with perturbed conformation could not tether platelets at high shear rates but promoted stable adhesion at lower shear and bound tightly to GP Ibα. Only in the presence of the exogenous modulator, botrocetin, did cyclic *r*vWF$^{445–733}$ mediate irreversible adhesion. Thus, conformational transitions in the vWF A1 domain may influence differentially the efficiency of bond formation with GP Ibα and the stability of binding.

The A1 domain of von Willebrand factor (vWF)[1] immobilized onto exposed surfaces at sites of vascular injury initiates platelet adhesion and thrombus formation by interacting with the glycoprotein (GP) Ibα receptor (1–3). This function is absolutely required for hemostasis in vessels such as arterioles or arterial capillaries, where rapid blood flow creates high shear rates (4, 5), and may also precipitate thrombosis in larger arteries, for example the coronary arteries of the heart, particularly at sites of stenosis caused by atherosclerotic lesions (6–8). The efficient interaction between GP Ibα and immobilized vWF is in apparent contrast to the lack of measurable binding of soluble plasma vWF (9). This observation has led to the generally accepted concept that conformational changes induced by surface adsorption regulate A1 domain function. Such an effect is thought to be caused *in vivo* by binding to collagen (10–12) or other subendothelial structures (13, 14), whereas *in vitro* it may be mimicked by interaction with modulators such as ristocetin (15, 16) or botrocetin (17–19). Indeed, surface-bound vWF may change shape under the influence of high shear stress, appearing as an elongated filament (20) rather than the loosely coiled structure predominantly seen under static conditions (21). Extended multimers expose repeating functional sites, thus supporting multiple and more efficient adhesive interactions. Whether the change in molecular shape parallels specific conformational transitions in the A1 domain is unknown at present. Nevertheless, physicochemical modifications of the isolated A1 domain in solution can result in heightened interaction with GP Ibα (22), in agreement with the notion that the native conformation is functionally unfavorable for receptor recognition but can be positively modulated. Consequently, it is generally assumed that the mechanisms leading to soluble vWF binding to GP Ibα reflect conditions that endow the A1 domain with the ability to initiate platelet adhesion.

The physiologic characteristics of the interaction between surface-immobilized vWF A1 domain and GP Ibα have been well established under relevant flow conditions, with the demonstration that the process supports efficient tethering even at high shear rates. Platelets kept in contact with the surface by this ligand receptor pairing, however, are not irreversibly adherent; rather, they translocate constantly in the direction of flow albeit at a markedly reduced velocity relative to freely flowing platelets (1). This is sufficient to allow the formation of additional bonds, mediated by receptors other than GP Ibα, resulting in irreversible attachment and subsequent thrombus formation (3). We have now studied the GP Ibα-binding function of isolated recombinant A1 domain fragments of distinct conformation to evaluate how adhesive properties under flow correlate with the ability to bind to the receptor in solution. We found that an immobilized fragment with refolded conformation supported platelet tethering at high shear rates as efficiently as native vWF but had the lowest GP Ibα binding capacity in solution. In contrast, disruption of the tertiary structure (22) resulted in a fragment that exhibited markedly enhanced binding to the receptor in solution, as judged by the ability to block its function, but defective support of platelet adhesion when immobilized onto a surface, particularly at high shear rates. Moreover, platelets became irreversibly attached to the fragment with disrupted conformation, rather than translocating through transient interactions as seen with native refolded fragments and multimeric vWF. After forming a complex with botrocetin, however, even A1 domain fragments with native conformation supported irreversible adhesion. Our findings indicate that the affinity regulation of vWF A1 domain

* This work was supported in part by Grants HL-31950, HL-42846, and HL-48728 from the National Institutes of Health. The costs of publication of this article were defrayed in part by the payment of page charges. This article must therefore be hereby marked "*advertisement*" in accordance with 18 U.S.C. Section 1734 solely to indicate this fact.

‡ Present address: Dept. of Blood Transfusion Service, National Cardiovascular Center, 7-1 Fujishirodai 5-chome, Suita, Osaka 565-8565, Japan.

§ To whom correspondence should be addressed: Dept. of Molecular and Experimental Medicine, SBR-8, The Scripps Research Institute, 10550 North Torrey Pines Rd., La Jolla, CA 92037. Tel.: 619-784-8950; Fax: 619-784-2026; E-mail: ruggeri@scripps.edu.

[1] The abbreviations used are: vWF, von Willebrand factor; GP, platelet membrane glycoprotein; PPACK, D-phenyl alanyl-L-prolyl-L-arginine chloromethyl ketone dihydrochloride.

binding to GP Ibα is a complex event since distinct and, in most instances, mutually exclusive structural characteristics control the ability to establish stable bonds or to initiate platelet tethering opposing elevated shear forces.

EXPERIMENTAL PROCEDURES

Preparation of Reconstituted Blood—Blood was collected from healthy and medication-free donors into polypropylene syringes containing as anticoagulant the α-thrombin inhibitor D-phenylalanyl-L-prolyl-L-arginine chloromethyl ketone dihydrochloride (PPACK) at the final concentration of 50 μM. All human subjects participating in these studies were aware of the experimental nature of the research and gave their informed consent in accordance with the Declaration of Helsinki. In order to eliminate potential effects of vWF and/or other plasma proteins in the experiments to be performed, washed blood cells suspended in perfusion buffer were prepared as follows. After adding the ADP scavenger apyrase and prostaglandin E_1 to prevent platelet activation (10 units/ml and 10 μM, respectively, final concentration), blood was centrifuged at 2200 × *g* for 15 min at room temperature (22–25 °C), and the resultant supernatant plasma was removed from the sedimented cells, including platelets and leukocytes on top of the erythrocyte cushion. After adding an equivalent volume of divalent cation-free Hepes/Tyrode buffer (10 mM Hepes, 140 mM NaCl, 2.7 mM KCl, 0.4 mM NaH_2PO_4, 10 mM $NaHCO_3$, and 5 mM dextrose), pH 6.5, and mixing gently, the cell suspension was centrifuged again and the supernatant fluid was removed. This procedure was repeated three additional times, and after the final centrifugation the cells were suspended in divalent cation-free Hepes/Tyrode buffer, pH 7.4, containing 50 mg/ml bovine serum albumin. Final cell counts were within normal blood limits. In some experiments, platelet-depleted reconstituted blood was prepared by centrifuging the final cell suspension at 150 × *g* for 15 min, removing the resulting platelet-rich supernatant fluid, and replacing it with an equivalent volume of Hepes/Tyrode buffer, pH 7.4, containing 50 mg/ml bovine serum albumin. After counting the platelet number in both the whole cell suspension and the platelet-rich suspension, appropriate volumes of the latter were added into the former to obtain the target platelet count in the reconstituted blood, at the same time maintaining a normal hematocrit. In some experiments, whole blood containing PPACK as anticoagulant and prostaglandin E_1 to prevent platelet activation (see above) was used instead of reconstituted blood.

Preparation of Purified Native vWF and Recombinant Fragments Containing the vWF A1 Domain—Native multimeric vWF was purified as previously reported (23). Two recombinant polypeptides coding for residues 508–704 and 445–733 of the mature vWF subunit, designated *r*vWF$^{508–704}$ and *r*vWF$^{445–733}$, respectively, were expressed in host *Escherichia coli* BL21-DE3 using plasmids containing the T7 RNA polymerase promoter (24, 25) and induction with isopropyl-β-D-thiogalactopyranoside, as described previously in detail (22, 26, 27). To prevent formation of random aggregates during purification, five codons for Cys residues at positions 459, 462, 464, 471, and 474 in the *r*vWF$^{445–733}$ construct were replaced with Gly codons by site-directed mutagenesis. Expressed fragments were purified by reverse-phase high pressure liquid chromatography and subjected either to reduction and alkylation (*S*-carboxyamidomethylation) or oxidization of the two Cys residues at positions 509 and 695, according to previously described procedures (22). Oxidization created the intramolecular disulfide bond that exists in native plasma vWF (28). Purified recombinant fragments were dialyzed against 2 mM acetic acid titrated to pH 3.5 with HCl and stored at −70 °C. As reported in detail elsewhere (22), refolding of the oxidized recombinant fragments from the denatured state following exposure to acidic pH was achieved by slow dialysis with incremental pH increase in steps of 0.5 units each up to a final value of 7.0 for *r*vWF$^{508–704}$ or 5.0 for *r*vWF$^{445–733}$. This was obtained by dialyzing the samples at 4 °C against 2 mM acetic acid to which an appropriate amount of ammonium hydroxide was added every 8 h. Limiting the pH for refolding *r*vWF$^{445–733}$ was necessary because this fragment tended to form aggregates at pH values above 5.0. Reduced and alkylated *r*vWF$^{508–704}$ was not refolded slowly, rather it was rapidly returned to neutral pH just before use by direct mixing with an appropriate buffer. Protein concentration was determined with the micro BCA assay (Pierce) according to the instructions of the manufacturer.

Purification of Two-chain Botrocetin—This modulator of vWF A1 domain binding to platelet GP Ibα was purified from the venom of the snake *Bothrops jararaca* as previously reported in detail (29, 30). It was stored in Hepes buffer (10 mM Hepes, 140 mM NaCl), pH 7.4, at −70 °C until used.

Monoclonal Antibodies—The anti-vWF, anti-GP Ibα, and anti-$\alpha_{IIb}\beta_3$ (GP IIb-IIIa) monoclonal antibodies used in these studies have been characterized in previous publications. Pooled M13 monoclonal antibodies (31, 32) recognize epitopes in the M13 cyanogen bromide fragment of vWF comprising residues 631–710 of the mature subunit (33). NMC-4 (34) recognizes a defined epitope in the A1 domain of vWF, as demonstrated by atomic structure resolution (35). LJ-Ib1 reacts with the amino-terminal 45-kDa domain of GP Ibα (36, 37) and is a competitive inhibitor of vWF binding to this platelet receptor. LJ-CP8 is a complex specific antibody against the integrin $\alpha_{IIb}\beta_3$ and completely blocks binding of all ligands to this receptor (38, 39). All monoclonal antibodies were mouse IgG_1 and were purified by protein A-Sepharose (Amersham Pharmacia Biotech) chromatography according to published procedures (40). The inhibitory effect of specific monoclonal antibodies on platelet interaction with immobilized native vWF or recombinant fragments was assessed by incubating purified IgG with reconstituted blood at room temperature for 20 min before perfusion through the chamber.

Assessment of the Interaction between Soluble Recombinant vWF Fragments and GP Ibα as Measured by Inhibition of the Anti-GP Ibα Monoclonal Antibody LJ-Ib1 Binding to Platelets—This assay, an indirect measurement of the binding to platelet GP Ibα of recombinant vWF fragments containing the A1 domain, has been described in detail in a previous publication (22). Platelet-rich plasma was prepared by centrifugation of blood containing PPACK at 150 × *g* for 15 min at room temperature and then diluted in 10 mM Hepes buffer, pH 7.4, to give a final platelet count of 1×10^8/ml. In other experiments, washed cells were prepared as described above, and a plasma-free suspension of platelets was obtained by centrifuging the final cell suspension at 150 × *g* for 15 min yielding a platelet-rich supernatant fluid that could be separated from the sedimented red and white blood cells. A constant volume (equal to or less than 12.5 μl) of various concentrations of each recombinant vWF fragment was added to the platelet suspension, followed by 10 μg/ml ^{125}I-labeled LJ-Ib1 (a concentration of antibody resulting in half-maximum binding to platelets) diluted in 10 mM Hepes buffer, pH 7.4. When indicated, botrocetin was also added to a final concentration of 5 μg/ml (0.17 μM); in this case, washed platelets (41) were used rather than platelet-rich plasma. The final volume of each experimental mixture was 125 μl, and all indicated concentrations were final. After incubation at room temperature for 30 min, platelets were separated by centrifugation though a layer of 20% sucrose, and bound radioactivity was measured in a γ-scintillation counter. Nonspecific binding was estimated by adding a 100-fold excess of nonlabeled LJ-Ib1, and the corresponding value (always less than 10% of the total counts added) was subtracted from all data points. Binding was expressed as percentage of that measured in a control mixture containing, instead of a recombinant vWF fragment, 12.5 μl of 10 mM ammonium acetate with the same pH.

Preparation of Glass Coverslips Coated with Immobilized Protein—Recombinant vWF fragments and native vWF were diluted to a final concentration of 100–130 μg/ml with 2 mM ammonium acetate, pH 7.0. A glass coverslip (number 1, 24 × 50 mm; Corning) was coated evenly with 200 μl of protein solution and placed in a humid environment at room temperature for 1 h. In some experiments, larger volumes (300–600 μl) of solutions with lower protein concentration were used. Just before assembly of the flow chamber, unbound protein was removed by rinsing the surface of the coverslip with 0.04 M phosphate buffer, pH 7.4, containing 0.15 M NaCl (PBS, phosphate-buffered saline composed of 0.04 M monosodium phosphate and 0.04 M disodium phosphate with 0.15 M NaCl, pH 7.4). In some cases, after coating with the desired protein, the glass surface was saturated with a solution of 50 mg/ml bovine serum albumin in PBS for 1 h at room temperature before use. To calculate the amount of protein adsorbed onto the glass surface, the supernatant containing unbound protein was carefully recovered after coating as were three successive 200-μl aliquots of PBS used to rinse the coverslip (washing solution). The amount of adsorbed protein was calculated as the difference between the total amount added for coating and that recovered in the coating plus washing solutions.

Flow Chamber and Perfusion Studies—Platelet interaction with immobilized recombinant fragments or native vWF under flow conditions was observed in real-time by means of epifluorescence videomicroscopy in a modified Hele-Shaw flow chamber (42), as described previously (1, 3). The bottom of the chamber was formed by the protein-coated surface of a glass coverslip, and a flow path height of 254 μm was determined by a silicon rubber gasket designed with a shape that resulted in a linear variable wall shear rate from 1500 s^{-1} at the inlet to 50 s^{-1} near the outlet when the flow rate was maintained at 2 ml/min. The entire flow path of the chamber, mounted on the stage of an inverted epifluorescence microscope (Axiovert 135 M, Carl Zeiss Inc.), was kept at 37 °C with a thermostatic air bath. Platelets were visualized by adding me-

TABLE I

Amount of native multimeric vWF and recombinant vWF fragments absorbed onto the surface of glass coverslips

The amount of protein adsorbed onto the surface of glass coverslips was determined by subtracting from the total initial amount in the coating solution the sum of that recovered in the supernatant solution after coating and in all washing solutions.

Protein	Coating solution		Supernatant		Washing solution		Density of protein
	Volume	Concentration	Volume	Concentration	Volume	Concentration	
	μl	μg/ml	μl	μg/ml	μl	μg/ml	μg/coverslip
1st experiment							
Native vWF	200	128	150	106	510	1.7	8.8
*r*vWF$^{445–733}$ cyclic	200	134	155	51	570	6.4	15.2
*r*vWF$^{508–704}$ cyclic	200	121	145	72	530	0.8	13.5
*r*vWF$^{508–704}$ R/A	200	123	163	75	575	1.8	11.3
2nd experiment							
Native vWF	200	128	155	100	580	2.3	8.7
*r*vWF$^{445–733}$ cyclic	200	134	155	55	580	8.7	13.3
*r*vWF$^{508–704}$ cyclic	200	121	150	73	570	0.5	13.1
*r*vWF$^{508–704}$ R/A	200	123	162	73	573	1.9	11.7

pacrine (quinacrine dihydrochloride; 10 μM final concentration), a fluorescent dye that becomes concentrated in the dense granules and has no effects on function at the concentration used (43). When native vWF was immobilized on the surface, reconstituted blood also contained the anti-$\alpha_{IIb}\beta_3$ monoclonal antibody, LJ-CP8, at the final concentration of 50 μg/ml in order to eliminate any irreversible interaction between platelets and the RGD sequence in vWF (1, 3). In some experiments, recombinant vWF fragments were mixed with the reconstituted blood to evaluate their capacity to inhibit, when in solution, the interaction of platelets with immobilized native vWF or recombinant fragments adsorbed onto the surface. Reconstituted blood, considered to have the same viscosity of 4 centipoise as native blood, was aspirated through the chamber, initially filled with PBS, by a syringe pump (Harvard Apparatus Inc.) for the desired time, and all experiments were continuously recorded on videotape using a video cassette recorder (VCR, Magnavox).

Analysis of Platelet Interaction with Native vWF and Recombinant vWF Fragment Immobilized onto a Glass Surface—The number of individual platelets interacting at any given time with immobilized native vWF or recombinant fragments was measured on images obtained at different positions in the flow path of the chamber, corresponding to selected wall shear rates. Each image corresponded to a single frame from the real time (30 frames/s) videotape recording, digitized and processed by computer analysis using a Sony 9500 VCR, a Matrox Image LC frame grabber, and the MetaMorph software package (Universal Imaging Corp.). The motion of platelets not irreversibly attached to the surface was analyzed as previously reported (1, 3). To evaluate the number of platelets displaced from the point of initial interaction, a series of images at 1/3–1/15-s intervals from real time recording was digitized and binarized after application of a threshold to distinguish platelets from background. Movement was defined as spatial displacement on the surface greater than one platelet diameter. The first two consecutive frames in the series were superimposed by the logical AND function, so that the resultant image represented only overlapping areas of an individual platelet at two different times. This computed image was then superimposed to next frame in the time series, and the same logical AND function was applied. The process was repeated for a number of frames corresponding to a preselected time interval, or until the area of overlap was equal to 0. When the latter occurred, the platelet had moved by a distance greater than its diameter; if this did not occur, the platelet was considered firmly attached during the period of observation. To measure the velocity of translocation onto the surface, the centroid of individual platelets on each image was assigned a set of x and y coordinate values. Centroid displacement was then followed as a function of time, typically on a total of 60 frames for each analyzed position in the chamber corresponding to 4–20 s. The rate of frame acquisition from real time recording was selected in relation to the speed of translocation. The velocity of individual platelets was calculated as the distance traveled by the centroid divided by the time interval (1, 3).

RESULTS

Coating of vWF A1 Domain Fragments onto a Glass Surface—Preliminary experiments established that platelet adhesion to immobilized native vWF or recombinant fragments was maximal after coating glass with a solution at the concentration of 100 μg/ml for 1 h at room temperature (22–25 °C). The corresponding amount of bound protein was in the range of 8.7–15.2 μg per glass slide for all recombinant fragments as well as purified native vWF (Table I). The number of platelets interacting with the coated surface was directly correlated to the amount of adsorbed protein, but considerably less native multimeric vWF than recombinant fragment was required for maximum effect (Fig. 1).

Platelet Interaction with Immobilized A1 Domain Fragments of Distinct Conformation—Platelet interaction with immobilized recombinant fragments as well as native multimeric vWF was evaluated in real time at wall shear rates between 50 and 6000 s^{-1}. Fragments of different conformation exhibited considerable variation in their ability to support platelet attachment (Fig. 2). Immobilized *r*vWF$^{445–733}$, refolded after oxidation of the Cys^{509}-Cys^{695} intrachain disulfide bond, interacted with platelets at all shear rates tested in a manner indistinguishable from multimeric vWF. As with the native molecule, the surface coated with this fragment became saturated with interacting platelets within seconds from the initiation of perfusion. In contrast, the shorter *r*vWF$^{508–704}$ with oxidized intrachain disulfide bond was efficient in interacting with platelets at shear rates up to 1500 s^{-1} but exhibited progressive loss of function with increasing shear and was essentially inactive at 6000 s^{-1} (Fig. 2). The same *r*vWF$^{508–704}$, but with reduced and alkylated Cys residues and brought from acidic to physiologic pH just before coating onto glass, supported the attachment of fewer platelets and only at the lower shear rates tested (Fig. 2). Real time images of platelets interacting with different immobilized substrates are shown in Fig. 3.

Analysis of Platelet Motion on Immobilized Native vWF and A1 Domain Fragments—The distinctive features of GP Ibα-mediated platelet interaction with immobilized vWF A1 domain are efficient initial tethering even at elevated wall shear rates (Fig. 2) and continuous surface translocation mediated by rapidly forming but transient bonds (Fig. 4). Motion on the surface, defined as displacement from the point of initial contact greater than one platelet diameter, occurred with nearly identical time course on native vWF and *r*vWF$^{445–733}$ cyclic at both relatively high (1500 s^{-1}) or low (340 s^{-1}) wall shear rates (Fig. 4). Within less than 5 s, essentially all the platelets that became tethered to either substrate were displaced from the point of first contact, but many remained attached to the surface for as long as they could be visualized, moving at a velocity dependent to some extent on the flow rate. Nevertheless, these platelets failed to arrest permanently as long as their interaction with the surface was mediated only by GP Ibα binding to native vWF A1 domain (Fig. 4). In remarkable contrast, when platelets were perfused over immobilized *r*vWF$^{508–704}$ with

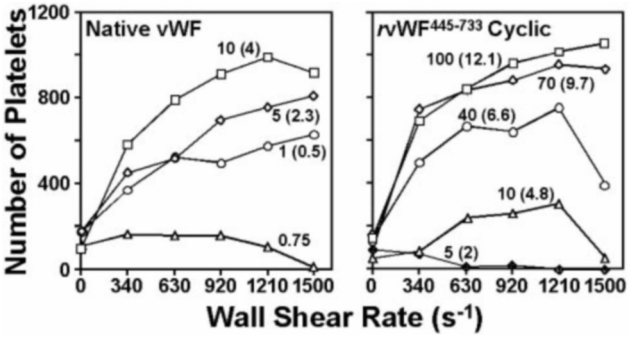

FIG. 1. **Effect of immobilized ligand density on the number of surface interacting platelets.** Reconstituted blood with mepacrine-labeled platelets was perfused at 37 °C through a Hele-Shaw chamber at a constant flow rate such that the indicated wall shear rates were attained at set positions on the *x-y* axes (see "Experimental Procedures"). The bottom of the chamber was formed by a glass coverslip coated with either native multimeric vWF (*left panel*) or *r*vWF$^{445–733}$ cyclic (*right panel*). The amount of surface-immobilized ligand per glass coverslip (surface area of 1200 mm^2) was measured as described in Table I and is indicated in *parentheses* after the corresponding concentration in the coating solution for each experiment performed. The amount of immobilized ligand at the lowest vWF coating concentration was too low to be determined accurately. The number of surface interacting platelets was measured after 2 min from the beginning of flow on single frames from real time recording and represents instantaneous (1/30th of a second) surface coverage including both transiently interacting and firmly attached platelets in an area of 65,536 μm^2.

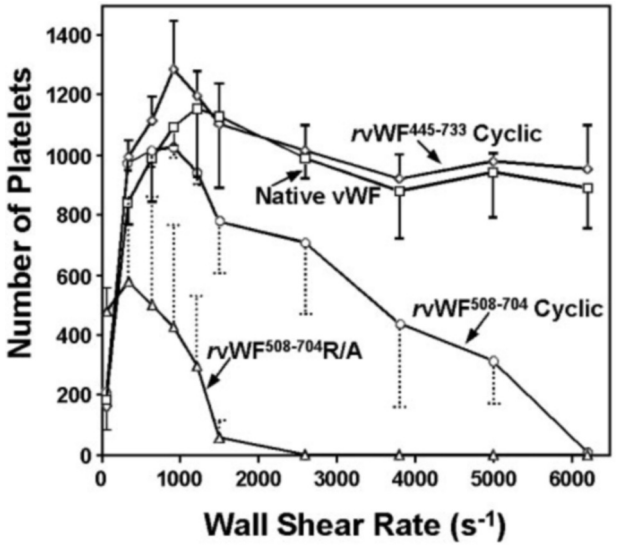

FIG. 2. **Effect of wall shear rate on platelet interaction with immobilized native vWF and different recombinant vWF fragments containing the A1 domain.** Reconstituted blood was perfused in a Hele-Shaw chamber, as described in the legend to Fig. 1, over glass coverslips coated with saturating amounts (100 μg/ml in the coating solution) of the indicated substrates (*R*/*A* indicates the fragment with reduced and alkylated Cys residues). Two different flow rates were used, one to evaluate wall shear rates between 50 and 1500 s^{-1} and the other between 2,000 and 6,000 s^{-1}. After 2 min of perfusion monitored in real time and recorded on video tape, single frame images from different positions in the chamber corresponding to the indicated wall shear rates were analyzed to measure the number of platelets interacting with the surface in an area of 65,536 μm^2. Each experimental point represents the mean ± S.D. of three separate experiments.

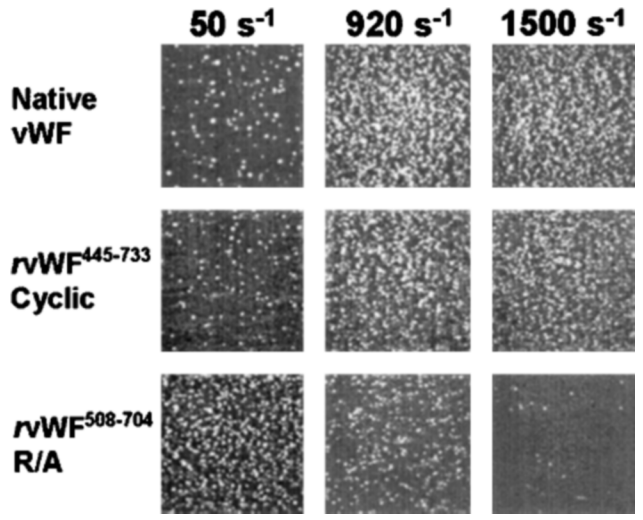

FIG. 3. **Images of surface-interacting platelets.** These images of single frames from real time recording show single platelets, appearing as individual bright spots, either permanently attached or transiently interacting with glass surfaces coated with the indicated substrates (see Fig. 2). Each frame represents an instantaneous (1/30th of a second) view of a 65,536-μm^2 surface area at three different wall shear rates.

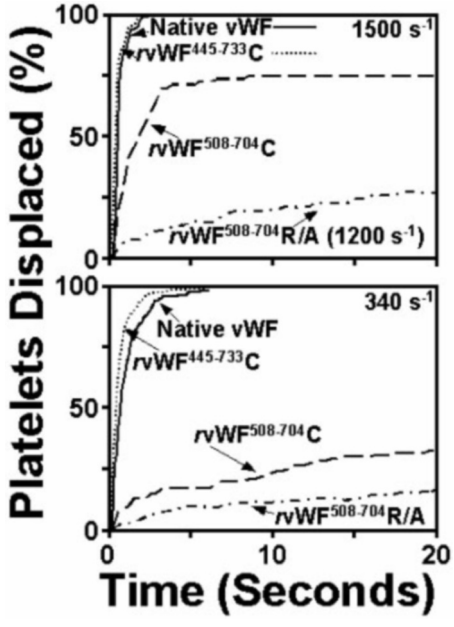

FIG. 4. **Analysis of platelet motion mediated by interaction with immobilized native vWF or different recombinant vWF fragments containing the A1 domain.** Platelet interaction with immobilized native vWF or the indicated recombinant fragments was observed and recorded in real time as described in the legend to Fig. 1 (*C* = fragment with oxidized Cys residues; *R*/*A* = fragment with reduced and alkylated Cys residues). After 2 min of perfusion, platelet motion on the surface was analyzed as described under "Experimental Procedures." Platelets whose centroid moved from the point of first contact by more than their own diameter were considered to be displaced and are reported as percentage of the total number of individual platelets that could be visualized on the surface during the observation period. Platelets that were not displaced according to this definition for more than 20 s were considered to be permanently adherent. *Upper panel,* perfusion at 1500 s^{-1}, except for the fragment *r*vWF$^{508–704}$ with reduced and alkylated Cys residues that was tested at the highest shear rate of 1200 s^{-1} owing to its decreased ability to initiate platelet tethering to the surface (see Fig. 2). *Lower panel,* perfusion at 340 s^{-1}.

reduced and alkylated Cys residues (R/A), initial tethering resulted in arrest at the site of first contact in greater than 70% of events at either relatively high or low shear rates (Fig. 4). Note that only for this fragment the highest shear rate for evaluation of surface translocation was 1200 s^{-1}, since initial tethering was extremely reduced at higher values (Fig. 2). The functional properties of *r*vWF$^{508–704}$ were considerably different when Cys^{509} and Cys^{695} were linked in intrachain bond, and the protein was refolded before use. On such a substrate, greater than 70% of initially tethered platelets attached irreversibly at the site of first contact at the lower shear rate of 340

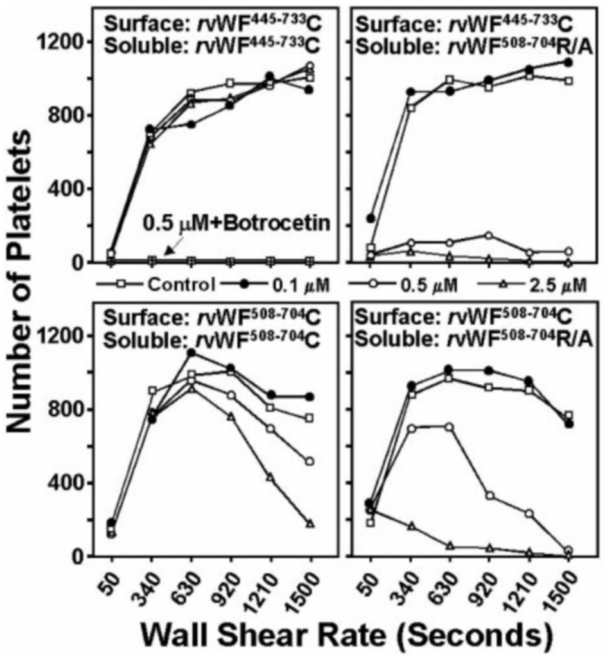

FIG. 5. **Platelet adhesion to immobilized cyclic (*C*) vWF fragments containing the A1 domain and inhibition by homologous fragments in solution either cyclic or with reduced and alkylated (R/A) Cys residues.** The indicated soluble recombinant vWF fragments were added into reconstituted blood at room temperature for 20 min before perfusion through the chamber. The different final concentrations tested are identified by distinct symbols (*control* = no soluble fragment added). Inhibitory activity was evidenced by a decrease in the number of platelets interacting with the immobilized fragments on the surface. Measurements were performed over an area of 65,536 μm^2, regardless of whether platelets were moving or firmly attached. Note (*upper left panel*) that even soluble *r*vWF$^{445–733}$, a noninhibitory fragment by itself, could completely prevent platelet adhesion after forming a complex with 0.5 μM botrocetin in solution.

s^{-1}, but only approximately 25% did so at 1500 s^{-1}, and the remaining 75% showed surface translocation (Fig. 4). Thus, it is apparent that conformational changes influenced by the presence or absence of the Cys^{509}-Cys^{695} disulfide bond in the vWF A1 domain are reflected both in the ability to support initial platelet-surface contacts, particularly at higher shear rates (Fig. 2), and in the stability of binding to GP Ibα.

Inhibition of Platelet Interaction with Immobilized Recombinant vWF Fragments by Homologous Species in Solution—Platelet adhesion to immobilized vWF fragments containing the A1 domain was inhibited to variable extent by homologous species in solution. Notably, *r*vWF$^{455–733}$ cyclic, the fragment that exhibited function similar to native vWF with respect to mediating platelet tethering and continuous translocation onto a surface (see Figs. 2 and 4), had essentially no ability to inhibit these processes even when present in excess amounts in solution (Fig. 5). In contrast, *r*vWF$^{508–704}$ with reduced and alkylated Cys residues, the fragment with markedly reduced ability to mediate initial platelet tethering but capable of supporting stable adhesion rather than translocation of platelets (see Figs. 2 and 4), could completely inhibit platelet interaction with both immobilized *r*vWF$^{455–733}$ and *r*vWF$^{508–704}$ cyclic (Fig. 5). The latter, when in solution, could inhibit platelet adhesion to the identical fragment immobilized onto a surface but only at the higher shear rates and concentrations tested (Fig. 5). The fact that these fragments in solution had different ability to bind to GP Ibα was confirmed by measuring the capacity to block binding to platelets of the monoclonal anti-GP Ibα antibody, LJ-Ib1 (Table II). Thus, it is apparent that conformational changes within the A1 domain of vWF can enhance its capacity

TABLE II

Inhibitory effect of different recombinant vWF fragments on the binding of the monoclonal antibody LJ-Ib1 to platelet glycoprotein Ibα

The anti-GP Ibα monoclonal antibody, LJ-Ib1, and vWF are competitive inhibitors for binding to platelets (22). Thus, the concentration (in μmol/liter) of recombinant vWF fragments containing the A1 domain required to inhibit by 50% the binding to platelets of the antibody LJ-Ib1 (IC_{50}) is inversely correlated to the affinity for GP Ibα. The reported values are the mean ± S.D. of 4–7 assays for each fragment tested.

Recombinant vWF fragment	IC_{50}
	μM
*r*vWF$^{445–733}$ cyclic	5.284 ± 2.216
*r*vWF$^{508–704}$ cyclic	1.165 ± 0.528
*r*vWF$^{508–704}$ reduced/alkylated	0.029 ± 0.006

to block GP Ibα in solution but at the expense of a decrease in the normal function of tethering platelets to a surface under high flow conditions. These results suggest that structural modifications reducing the dissociation rate of the interaction between vWF A1 domain and GP Ibα, a feature required for good inhibitory function in solution, may result in a slower association rate with consequent decreased efficiency in initiating platelet adhesion.

Effect of Complex Formation with Botrocetin on the Function of the A1 Domain Containing rvWF$^{445–733}$ Cyclic—The GP Ibα-binding activity of the vWF fragment *r*vWF$^{445–733}$ with oxidized Cys^{509}-Cys^{695} intrachain disulfide bond was modulated by botrocetin. As judged by competitive inhibition of monoclonal antibody LJ-Ib1 binding to platelets in the absence of flow, the fragment in solution exhibited a 100-fold greater affinity for GP Ibα in the presence than in the absence of the modulator (Fig. 6). In perfusion studies, immobilized fragment in complex with botrocetin mediated adhesion of an increased number of platelets as compared with the fragment alone at all shear rates tested, and in either case the interaction was inhibited by blocking GP Ibα (Fig. 7). In striking contrast to the results obtained in the absence of botrocetin, however, addition of increasing amounts of the modulator to *r*vWF$^{445–733}$ before immobilization onto glass resulted in progressively more stable platelet adhesion. Thus, instead of continuous surface translocation, the majority of platelets interacting with *r*vWF$^{445–733}$-botrocetin complex in equimolar proportion became irreversibly attached at the point of first contact (Fig. 8). This effect of botrocetin resembles that seen after altering the structure of *r*vWF$^{508–704}$ by reducing and alkylating Cys residues (Fig. 4), but with the notable difference that the *r*vWF$^{445–733}$-botrocetin complex was efficient in tethering platelets even at high shear rates (Fig. 7).

DISCUSSION

The interaction between vWF A1 domain and GP Ibα is key for initiating platelet thrombus formation at sites of vascular injury exposed to fast flowing blood (1, 3). Our results indicate that this function is independent of stable ligand-receptor binding, since the latter event may take place after induction of distinct A1 domain conformations that are not compatible with efficient platelet recruitment at high shear rates. The tethering of fast flowing GP Ibα to surface-immobilized vWF A1 domain requires rapid interaction, whereas stable binding to immobilized or soluble vWF is favored by slow dissociation of formed bonds. The findings reported here imply that the association rate with GP Ibα is the crucial parameter for A1 domain function under conditions of high shear stress, whereas prolonged stability is not a relevant nor a sufficient feature of the bond. Such a concept is in agreement with the evidence that permanent platelet adhesion is mediated by integrins, but these receptors bind to the respective ligands with relatively slow

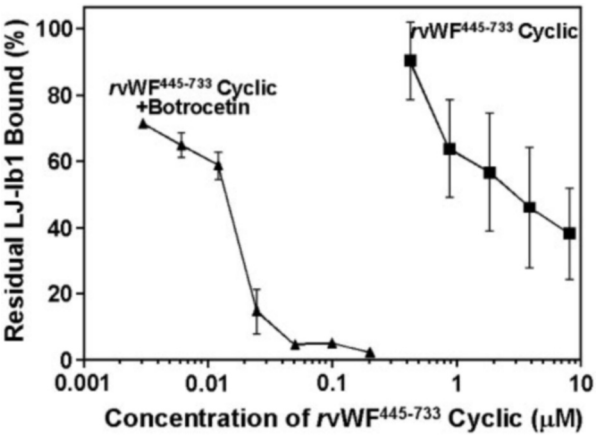

FIG. 6. **Effect of botrocetin on the inhibition of monoclonal antibody LJ-Ib1 binding to GP Ibα by soluble rvWF$^{445–733}$ cyclic.** Interaction of the recombinant vWF fragment with GP Ibα was evaluated indirectly by the ability to inhibit platelet binding of the specific monoclonal antibody LJ-Ib1. Platelet-rich plasma was mixed with refolded *r*vWF$^{445–733}$ cyclic, 10 μg/ml ^{125}I-labeled LJ-Ib1 IgG, and 10 mM HEPES buffer with 140 mM NaCl to give a final platelet count of 100,000/μl and the indicated final concentrations of reagents in a volume of 125 μl. When indicated, botrocetin was also added to a final concentration of 5 μg/ml (0.17 μM), but in this case washed platelets were used instead of platelet-rich plasma. After incubation at room temperature for 30 min, platelets were separated by centrifugation through a layer of 20% sucrose, and the radioactivity of bound LJ-Ib1 was measured in a γ-scintillation counter. Nonspecific binding was estimated with the addition of a 100-fold excess of nonlabeled antibody and was always <10% of total binding; the corresponding value was subtracted from all data points. Results are expressed as percentage of binding relative to a control mixture containing ^{125}I-labeled LJ-Ib1 IgG but no vWF fragment and are presented as mean ± S.D. (n = 4 for fragment alone; n = 2 for fragment + botrocetin). Addition of botrocetin without recombinant vWF fragment had no effect on antibody binding to platelets (not shown).

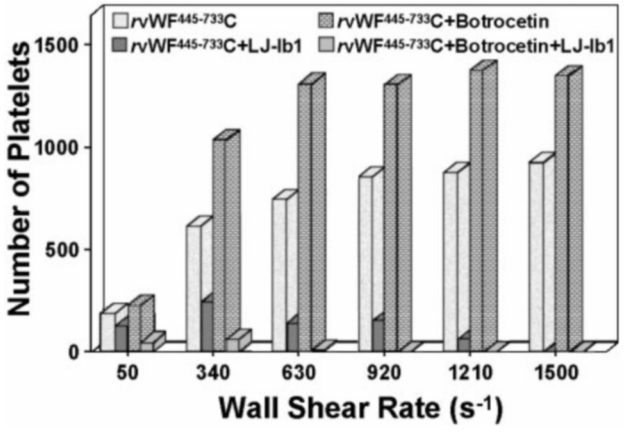

FIG. 7. **Platelet adhesion to rvWF$^{445–733}$ cyclic immobilized by itself or in complex with botrocetin.** Blood was perfused over glass coverslips coated with either *r*vWF$^{445–733}$ cyclic by itself (3 μM) or mixed with equimolar amounts of botrocetin. When indicated, the function blocking anti-GP Ibα monoclonal antibody LJ-Ib1 was added to the blood at the final concentration of 100 μg/ml (experiments without botrocetin) or 400 μg/ml (experiments with botrocetin). The higher concentration of antibody in the latter situation was necessary to achieve complete inhibition, owing to the fact that botrocetin enhances the apparent affinity of interaction between vWF A1 domain and GP Ibα, and LJ-Ib1 acts as a competitive inhibitor of ligand binding to the receptor. Perfusion at the indicated shear rates and evaluation of platelet adhesion was performed as described in the legend to Fig. 2.

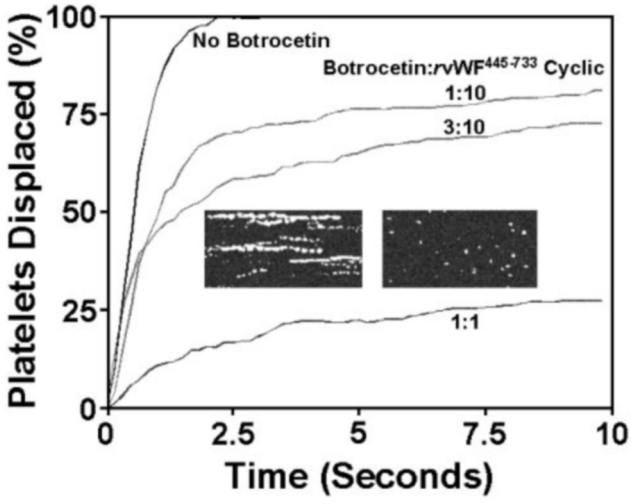

FIG. 8. **Analysis of the stability of platelet adhesion mediated by rvWF$^{445–733}$ cyclic immobilized by itself or in complex with botrocetin in various molar proportions.** The recombinant vWF fragment (3 μM) was mixed with botrocetin in the indicated molar proportions for 30 min at room temperature to allow for complex formation. The solution was then used to coat glass coverslips representing the reactive surface in perfusion experiments at the wall shear rate of 1,500 s^{-1}. Consecutive images from video tapes recorded in real time were captured at intervals of 1/3rd to 1/10th of a second, and the movement of individual platelets was followed as a function of time. Platelets showing spatial displacement on the surface greater than their own diameter were considered to be moving and are reported as percentage of the total number of individual platelets that could be visualized on the surface during the observation period. The *two insets* show platelets adhering to *r*vWF$^{445–733}$ cyclic alone (*left*) or in complex with botrocetin (*right*). Each image corresponds to a surface of 15,000 μm^2 and was created by superimposing 30 consecutive frames taken at intervals of one-third of a second from experiments recorded in real time (video rate of 30 frames per second); thus, a 3-s observation period is shown. The strings of fluorescent objects on the *left* result from the motion of single platelet tethered to the surface; the single round objects on the *right* reflect superimposition of platelets that did not move from the point of initial adhesion throughout the period of observation.

association rates and can be effective at high shear rates only after GP Ibα tethering to vWF (3). Platelet adhesion, therefore, results from the synergistic and coordinated function of several distinct interactions. In this context, critical to the role of vWF and GP Ibα is the balance of their "on" and "off" binding rates that must be tuned to support initial platelet attachment and transient arrest but without the need to establish stable bonds that are provided by other receptors (3). This appears to be best achieved by A1 domain conformations that allow rapid GP Ibα binding but retain intrinsically high dissociation rates. In fact, the two key parameters regulating the interaction seem to be modulated so that fast association and stable binding are mutually exclusive.

At present, it is generally assumed that the lack of measurable interaction between soluble plasma vWF and GP Ibα on circulating platelets is the expression of regulatory mechanisms needed to maintain ligand and receptor in the same environment without adverse consequences. Hence the notion that plasma vWF has a "nonfunctional" ("nonadhesive") conformation that must be switched to "functional" in order to initiate platelet adhesion, leading to the commonly accepted concept that a specific transition occurs upon adsorption of vWF onto appropriate substrates such as collagen. The results presented here, along with other published findings (3), suggest the possibility of a different scenario, since it is now apparent that A1 domain function in platelet adhesion does not necessarily associate with the ability to form stable interactions with GP Ibα. Thus, native vWF may potentially enable platelet tethering at sites of vascular injury even when no measurable binding to GP Ibα can be detected. Consequently, it may no longer be necessary to invoke a conformational change to explain the induction of vWF adhesive function. In this regard, attention has been paid to the effect of shear forces on the shape of vWF molecules. Transition from coiled forms in solution (21) to extended fila-

ments bound to substrates under fluid shear stress (20) may correlate to enhanced adhesive potential of vWF multimers, but a similar mechanism is unlikely to be relevant for isolated A1 domain fragments with tight globular shape (35). Yet, our results show an almost identical function of surface-bound vWF multimers and refolded A1 domain fragments in promoting efficient platelet tethering and rolling at high shear rates, as well as a similar inability of the soluble counterparts to interact significantly with GP Ibα. Thus, without the need for induction, the native A1 domain conformation may be set for receptor binding with high association and dissociation rates, a functional regulation that allows the molecule to support rapid platelet tethering at wound sites and, at the same time, to be nonreactive in blood.

The understanding that the functionality of vWF binding to GP Ibα depends on rapidity of bond formation but not stability in time (1, 3) provides new perspectives for defining the relevant aspects of A1 domain structure and function. An immediate and unrestricted response to vascular injury is clearly favored by the fact that plasma vWF is competent for binding to GP Ibα promptly after immobilization, without the need for induction by specific modulators. Such a feature, however, implies high dissociation rate from GP Ibα as a necessary property to allow the coexistence of platelets and vWF in blood, so that occasional interactions have limited lifetime and cause no functional consequences in the absence of other thrombogenic stimuli. The possibility of ligand-receptor contacts in blood is also minimized by the low plasma vWF concentration. Considering that each subunit contains one A1 domain, even a molar concentration 10-fold above the normal average would be well below the amount necessary to measure binding to GP Ibα in the absence of exogenous modulators (see Fig. 6). Moreover, the coiled shape of vWF in solution (21), shielding A1 domain sites, may further reduce the reactivity of the molecule. At least in this respect, therefore, molecular shape (20) is likely to have a role in regulating the consequences of vWF contact with platelets. In fact, multivalency contributes to efficient vWF interaction with GP Ibα, since a single multimer with extended shape is a cluster of A1 domains with the potential of forming multiple bonds concurrently. This explains why the surface density of isolated A1 domain must be considerably higher than that of the native multimeric ligand to support comparable interaction with platelets under flow.

The native conformation expressing the adhesive properties of intact vWF is maintained in a fragment with the carboxyl-terminal portion of domain D3 preceding domain A1. After oxidation of the Cys^{509}-Cys^{695} intrachain disulfide bond and refolding, such a molecule supports binding to GP Ibα with high association and dissociation rates, resulting in rapid platelet tethering at high shear rates but with continuous translocation and no permanent attachment. The native A1 domain conformation can be modulated to support stable platelet adhesion, reflecting decreased dissociation from GP Ibα, but acquisition of this property seems to be necessarily accompanied by less efficient platelet tethering at high shear rates, evidence for a concomitant decrease in the association rate. The functional transition occurs in molecules expressed without the portion of domain D3 preceding A1 and more markedly after reduction of the Cys^{509}-Cys^{695} disulfide bridge, suggesting that a less constrained conformation favors stability in A1 domain-GP Ibα bonds. In this regard, the consequences of complex formation with botrocetin (18, 44) are unique, in that irreversible binding to GP Ibα supporting permanent platelet adhesion is achieved without affecting recruitment at high shear rates. By analogy with the mechanism of platelet interaction with vWF bound to collagen or subendothelial matrix (3), the effect of botrocetin may be interpreted as the result of a contribution to the stability of binding, not of direct modulation of A1 domain activity. According to this alternative view, the two components of the vWF-botrocetin complex would act in sequence, initiating binding to GP Ibα through the intrinsically fast A1 domain association rate and providing additional contacts through botrocetin that essentially obliterate dissociation. Notable in this case is that both initial platelet tethering and permanent adhesion may be mediated by GP Ibα. A precedent suggesting the possibility of botrocetin participation in receptor binding can be found in the function of the highly homologous Jararaca GP Ib-BP (binding protein), a snake venom molecule with high affinity for GP Ibα (45). The significant difference may be that botrocetin cannot bind by itself but only contribute to the stability of the interaction initiated by the vWF A1 domain. It has been suggested that molecules functioning like botrocetin exist in the vessel wall (14), but mechanism of action and physiologic relevance of such a potential pathway of platelet thrombus formation remain to be established.

A relevant conclusion supported by the studies presented here is that A1 domain fragments with native conformation can mediate initial platelet-surface contacts as efficiently as multimeric vWF but have essentially no activity as soluble inhibitors of GP Ibα function. However, conditions have been defined to express modified A1 domain fragments that effectively block platelet adhesion to vWF at high shear rates. These results demonstrate the existence of mutually exclusive A1 domain conformations, one that can tether platelets in rapidly flowing blood but cannot form a lasting bond with GP Ibα, and one that mediates stable binding to the receptor but is poorly adhesive at high shear rates. Such considerations are relevant for a successful development of anti-thrombotic molecules interfering with the GP Ibα-vWF interaction. Indeed, an ideal candidate inhibitor should effectively block the platelet receptor with sufficient duration in time but should not become a possible substrate for platelet recruitment if adsorbed by subendothelial components exposed at sites of vascular injury. Achieving this goal may be facilitated by a detailed understanding of the structural bases regulating vWF A1 domain binding to GP Ibα, in particular by defining the residues specifically involved in determining association and dissociation rates of the interaction.

Acknowledgments—We thank James R. Roberts and Benjamin Gutierrez for preparing monoclonal antibodies; Richard A. McClintock for help with the purification and refolding of recombinant fragments; Dr. Brian Savage and Dr. Enrique Saldívar for assisting in the development of the methodology for flow experiments and image analysis. Support was provided by National Institutes of Health Grant RR0833 to the General Clinical Research Center of Scripps Clinic and Research Foundation and by the Stein Endowment Fund.

REFERENCES

1. Savage, B., Saldivar, E., and Ruggeri, Z. M. (1996) *Cell* **84,** 289–297
2. Ruggeri, Z. M. (1997) *J. Clin. Invest.* **99,** 559–564
3. Savage, B., Almus-Jacobs, F., and Ruggeri, Z. M. (1998) *Cell* **94,** 657–666
4. Tangelder, G. J., Slaaf, D. W., Arts, T., and Reneman, R. S. (1988) *Am. J. Physiol.* **254,** H1059–H1064
5. Goldsmith, H. L., and Turitto, V. T. (1986) *Thromb. Haemostasis* **55,** 415–435
6. Back, C. H., Radbill, J. R., and Crawford, D. W. (1977) *J. Biomech.* **10,** 339–353
7. Fuster, V., Badimon, L., Badimon, J. J., and Chesebro, J. H. (1992) *N. Engl. J. Med.* **326,** 242–250
8. Fuster, V., Badimon, L., Badimon, J. J., and Chesebro, J. H. (1992) *N. Engl. J. Med.* **326,** 310–318
9. Ruggeri, Z. M., and Ware, J. (1993) *FASEB J.* **7,** 308–316
10. Baumgartner, H. R., Tschopp, T. B., and Weiss, H. J. (1977) *Thromb. Haemostasis* **37,** 17–28
11. Pareti, F. I., Niiya, K., McPherson, J. M., and Ruggeri, Z. M. (1987) *J. Biol. Chem.* **262,** 13835–13841
12. Cruz, M. A., Yuan, H., Lee, J. R., Wise, R. J., and Handin, R. I. (1995) *J. Biol. Chem.* **270,** 10822–10827
13. de Groot, P. G., Ottenhof-Rovers, M., van Mourik, J. A., and Sixma, J. J. (1988) *J. Clin. Invest.* **82,** 65–73
14. Katayama, M., Nagata, S., Hirai, S., Miura, S., Fujimura, Y., Matusi, T., Kato,

I., and Titani, K. (1995) *J. Biochem.* (*Tokyo*) **117,** 331–338
15. Howard, M. A., and Firkin, B. G. (1971) *Thromb. Haemostasis* **26,** 362–369
16. Scott, J. P., Montgomery, R. R., and Retzinger, G. S. (1991) *J. Biol. Chem.* **266,** 8149–8155
17. Read, M. S., Shermer, R. W., and Brinkhous, K. M. (1978) *Proc. Natl. Acad. Sci. U. S. A.* **75,** 4514–4518
18. Read, M. S., Smith, S. V., Lamb, M. A., and Brinkhous, K. M. (1989) *Blood* **74,** 1031–1035
19. Sugimoto, M., Mohri, H., McClintock, R. A., and Ruggeri, Z. M. (1991) *J. Biol. Chem.* **266,** 18172–18178
20. Siediecki, C. A., Lestini, B. J., Kottke-Marchant, K., Eppell, S. J., Wilson, D. L., and Marchant, R. E. (1996) *Blood* **88,** 2939–2950
21. Fowler, W. E., Fretto, L. J., Hamilton, K. K., Erickson, H. P., and McKee, P. A. (1985) *J. Clin. Invest.* **76,** 1491–1500
22. Miyata, S., Goto, S., Federici, A. B., Ware, J., and Ruggeri, Z. M. (1996) *J. Biol. Chem.* **271,** 9046–9053
23. Ruggeri, Z. M., De Marco, L., Gatti, L., Bader, R., and Montgomery, R. R. (1983) *J. Clin. Invest.* **72,** 1–12
24. Studier, F. W., and Moffatt, B. A. (1986) *J. Mol. Biol.* **189,** 113–130
25. Rosenberg, A. H., Lade, B. N., Chui, D. S., Lin, S. W., Dunn, J. J., and Studier, F. W. (1987) *Gene* (*Amst.*)**56,** 125–135
26. Sugimoto, M., Dent, J., McClintock, R. S., Ware, J., and Ruggeri, Z. M. (1993) *J. Biol. Chem.* **268,** 12185–12192
27. Prior, C. P., Chu, V., Cambou, B., Dent, J. A., Ebert, B., Gore, R., Holt, J., Irish, T., Lee, J., Mitschelen, J., McClintock, R. A., Searfoss, G., Ricca, G. A., Tarr, C., Weber, D., Ware, J. L., Ruggeri, Z. M., and Hrinda, M. (1993) *BioTechnology* **11,** 709–713
28. Marti, T., Roesselet, S., Titani, K., and Walsh, K. A. (1987) *Biochemistry* **26,** 8099–8109
29. Fujimura, Y., Titani, K., Usami, Y., Suzuki, M., Oyama, R., Matsui, T., Fukui, H., Sugimoto, M., and Ruggeri, Z. M. (1991) *Biochemistry* **30,** 1957–1964
30. Usami, Y., Fujimura, Y., Suzuki, M., Ozeki, Y., Nishio, K., Fukui, H., and Titani, K. (1993) *Proc. Natl. Acad. Sci. U. S. A.* **90,** 928–932
31. Zimmerman, T. S., Dent, J. A., Ruggeri, Z. M., and Nannini, L. H. (1986) *J. Clin. Invest.* **77,** 947–951
32. Dent, J. A., Berkowitz, S. D., Ware, J., Kasper, C. K., and Ruggeri, Z. M. (1990) *Proc. Natl. Acad. Sci. U. S. A.* **87,** 6306–6310
33. Titani, K., Kumar, S., Takio, K., Ericsson, L. H., Wade, R. D., Ashida, K., Walsh, K. A., Chopek, M. W., Sadler, J. E., and Fujikawa, K. (1986) *Biochemistry* **25,** 3171–3184
34. Fujimura, Y., Usami, Y., Titani, K., Niinomi, K., Nishio, K., Takase, T., Yoshioka, A., and Fukui, H. (1991) *Blood* **77,** 113–120
35. Celikel, R., Varughese, K. I., Madhusudan, A., Yoshioka, A., Ware, J., and Ruggeri, Z. M. (1998) *Nat. Struct. Biol.* **5,** 189–194
36. Handa, M., Titani, K., Holland, L. Z., Roberts, J. R., and Ruggeri, Z. M. (1986) *J. Biol. Chem.* **261,** 12579–12585
37. Titani, K., Takio, K., Handa, M., and Ruggeri, Z. M. (1987) *Proc. Natl. Acad. Sci. U. S. A.* **84,** 5610–5614
38. Niiya, K., Hodson, E., Bader, R., Byers-Ward, V., Koziol, J. A., Plow, E. F., and Ruggeri, Z. M. (1987) *Blood* **70,** 475–483
39. Savage, B., Shattil, S. J., and Ruggeri, Z. M. (1992) *J. Biol. Chem.* **267,** 11300–11306
40. Ey, P. L., Prowse, S. J., and Jenkin, C. R. (1978) *Immunochemistry* **15,** 429–436
41. Goto, S., Salomon, D. R., Ikeda, Y., and Ruggeri, Z. M. (1995) *J. Biol. Chem.* **270,** 23352–23361
42. Usami, S., Chen, H. H., Zhao, Y., Chien, S., and Skalak, R. (1993) *Ann. Biomed. Eng.* **21,** 77–83
43. Dise, C. A., Burch, J. W., and Goodman, D. B. P. (1982) *J. Biol. Chem.* **257,** 4701–4704
44. Andrews, R. K., Booth, W. J., Gorman, J. J., Castaldi, P. A., and Berndt, M. C. (1989) *Biochemistry* **28,** 8317–8326
45. Kawasaki, T., Fujimura, Y., Usami, Y., Suzuki, M., Miura, S., Sakurai, Y., Makita, K., Taniuchi, Y., Hirano, K., and Titani, K. (1996) *J. Biol. Chem.* **271,** 10635–10639